Dissolution Characteristics of New Titanium Alloys in Electrochemical Machining

Chen Xuezhen, Zhu Dong, Xu Zhengyang, Liu Jia, Zhu Di*

College of Mechanical and Electrical Engineering, Nanjing University of Aeronautics and Astronautics, Nanjing 210016, P. R. China

(Received 15 May 2015; revised 3 October 2015; accepted 8 November 2015)

Abstract: We focus on the electrochemical dissolution characteristics of new titanium alloys such as near-α titanium alloy Ti60, α+β titanium alloy TC4 and β titanium alloy Ti40 which are often used for aerospace industry. The experiments are carried out by electrochemical machining tool, and the surface morphology of the specimens is observed by the scanning electron microscope (SEM) and three-dimensional video microscope (DVM). The appropriate electrolyte is selected and the relationships between surface roughness and current density are achieved. The results show that the single-phase titanium alloy Ti40 has a better surface roughness after ECM compared with the α+β titanium alloy TC4 and the near-α titanium alloy Ti60. The best surface roughness is Ra 0.28 μm when the current density is 75 A/cm^2. Furthermore, the surface roughness of the near-α titanium alloy Ti60 is the most sensitive with the current density because of the different electrochemical equivalents of substitutional elements and larger grains than TC4. Finally, the suitable current density for each titanium alloy is achieved.

Key words: electrochemical machining (ECM); titanium alloy; substitutional element; electrochemical equivalent; surface roughness

CLC number: TG662 **Document code**: A **Article ID**: 1005-1120(2016)05-0610-10

0 Introduction

Titanium alloys are widely used in the aeronautical industry because of their high strength, good corrosion resistance, excellent fatigue performance, and excellent strength-to-weight ratio[1-3]. The density of titanium is relatively low, and half that of steel. Its strength is not high, but after the addition of aluminum, vanadium, molybdenum, or other substitutional elements, titanium alloys attain high strengths that are as high as that of steel[4-6]. According to the organizational characteristics of titanium alloy by annealing, titanium alloy can be divided into three classes: α titanium alloy, β titanium alloy and α+β titanium alloy. For example, Ti60(Ti-5.6Al-2Zr-4.8Sn-1Mo-0.35Si-0.7Nd) is a new near-α high-temperature alloy and can be used for disks and blades of aircraft engines at about 600 ℃[7]. Ti40 (Ti-25V-15Cr-0.2Si) is a new β titanium alloy. Ti40 possesses good burn resistance and mechanical properties and has a wide range of possible applications, e.g. in the aerospace industry[8]. TC4 (Ti-6Al-4V) is a α+β titanium alloy and the most commonly used titanium alloy in the industry.

Electrochemical machining (ECM) is a non-traditional machining process, based on the principle of electrochemical dissolution of an anode in an electrolyte[9,10]. The process is carried out in an electrolytic cell, with the tool as the cathode and the workpiece as the anode, with controlled anodic electrochemical dissolution taking place when a voltage is applied between the workpiece and the tool[11-14]. ECM is one of the most potentially useful non-traditional machining processes because of its ability to machine complex and in-

* Corresponding author, E-mail address: xuzhy@nuaa.edu.cn.

How to cite this article: Chen Xuezhen, Zhu Dong, Xu Zhengyang, et al. Dissolution characteristics of new titanium alloys in electrochemical machining[J]. Trans. Nanjing Univ. Aero. Astro., 2016,33(5):610-619.
http://dx.doi.org/10.16356/j.1005-1120.2016.05.610

tricate shapes in high-strength and heat-resistant materials[15].

Some results in ECM of titanium alloys have been obtained. In India, Dhobe and his colleagues studied the surfaces of medical devices produced using ECM. The surface roughness *Ra* of an oxide-layered machined surface obtained was in the range 3.09—3.66 μm[16,17]. American investigators also conducted some research on ECM of medical devices[18]. TC4 has been studied in China, and the results show that a machining surface roughness *Ra* of 0.413 μm can be obtained with the use of an additional anode made of platinum in an electrolyte of 10 wt% NaCl + ethylenedia minetetraacetic acid(EDTA) + 4 wt% $Na_2S_2O_8$ at a current density of 50 A/cm^2[19]. In Germany, Klocke and his colleagues also conducted experimental investigations into ECM of modern titanium alloys for aero-engine components[20]. In the former Soviet Union, Shulepov and his colleagues investigated ECM of titanium alloy using a sectional cathode under conditions in which the current is applied intermittently[21].

Titanium alloys differ not only in composition, but also in microstructure. At present, in investigations of ECM of titanium alloys, the ECM parameters are obtained from a large number of orthogonal or uniform experiments but not from the elements and phases of the material. The current density has a significant effect on surface roughness. Traditionally, for stainless steel, the higher the current density is, within a certain interval, the better the surface roughness is[22]. However, for titanium alloys, this rule cannot always be applied. Meanwhile, the researches of the new titanium alloy Ti60 and Ti40 in ECM are less before.

In the paper, the experiment of the three different types of titanium alloy (Ti60, Ti40 and TC4) will be carried out. An appropriate electrolyte is selected, and a suitable current density is chosen for each alloy. By comparing different elements, type of phases and size of phases, the test results are further analyzed.

1 Experimental Preparation

1.1 Experimental equipment

The ECM system used in the experiments is shown schematically in Fig. 1. It consists of a number of precision-machined components: a filter press to remove byproducts, a heat exchanger to control the electrolyte temperature during ECM, and a fine filter to remove small-sized impurities during processing, together with auxiliary equipment to measure and control the flow rate. The electrolyte is pumped with the centrifugal pump 2 from the electrolyte tank and fed to the processing area. The throttle 1 mainly controls the flow rate in the processing area, with the remaining electrolyte returning to the electrolyte tank through the liquid return pipe. The flow meter and inlet pressure gauge measure the flow rate at the entrance to the processing area. To reduce flow field defects in the ECM area, back pressure is applied at the outlet region. The back pressure is controlled by throttle 2, and the outlet pressure gauge shows the value of the outlet pressure. The high-current electrical power supply is controlled by a programmable logic controller.

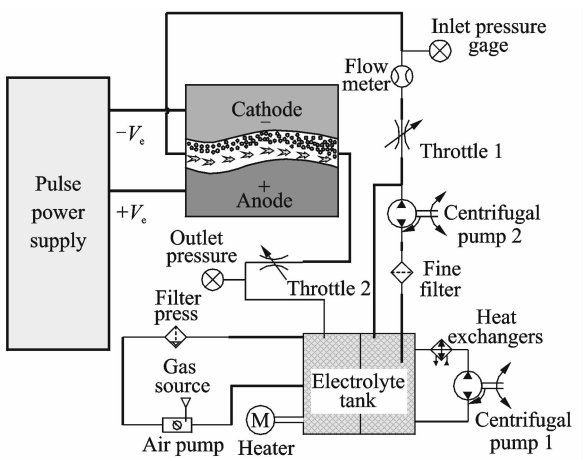

Fig. 1 Schematic diagram of ECM system

1.2 Steady flow field system for ECM

To obtain a good machined surface, a steady flow field system for ECM is developed independently of the present work. The main components of this system are a jig cover, a jig base, a cathode tool, an anode connecting rod, and a blank.

The jig cover, which has a slit at the bottom, is fixed to the jig base, which also has a slit, by locating pins and screws. The electrolyte flows from the slit at high speed. The diameter of the workpiece, which is held inside a specially designed hollow cylindrical anode connecting rod, is 20 mm.

To achieve a constant flow field without sharp corners (which can lead to the formation of cavities), the cathode tool is held stationary while the anode connecting rod moves toward the cathode at a pre-set speed. A schematic diagram of the flow field is shown in Fig. 2. The steady flow field system used for ECM in the present experiments is shown in Fig. 3.

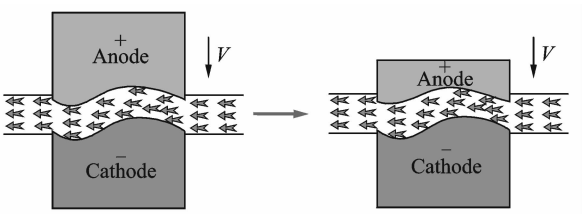

Fig. 2 Schematic diagram of flow field for anode feeding

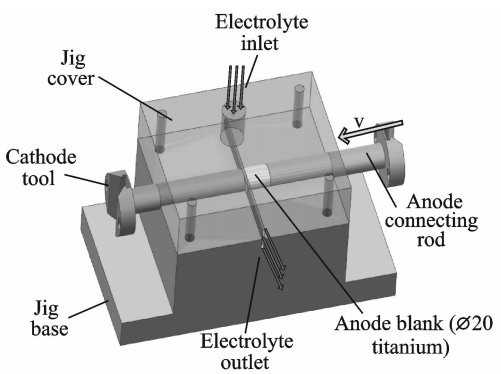

(a) Schematic diagram of system

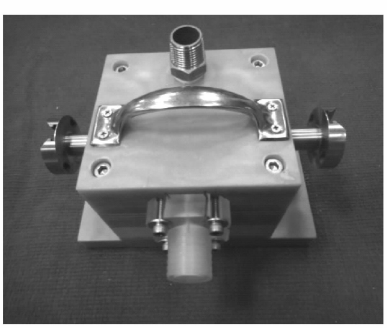

(b) Photograph of system

Fig. 3 Diagram and photograph of steady flow field system for ECM

1.3 Experimental materials

Ti60 is a near-α high-temperature alloy, and is applied in the blisk of the aero engine[7]. Furthermore, the α-phase stabilizer element (Al) is more concentrated in the α phase, and the β-phase stabilizer elements (Mo, Si) are more concentrated in the transformed β structure, while the neutral elements (Zr, Sn) are both easily dissolved in the two structures. The metallograph of Ti60 is shown in Fig. 4(a). The spherical part is primary α phase, and the strip structure with black border is transformed β structure which have secondary α phase and intergranular β phase.

TC4 is a α+β titanium alloy and is one of the most commonly used. The α phase and β phase are evenly distributed in the alloy. Furthermore, the α-phase stabilizer element (Al) is more concentrated in the α phase, while the β-phase stabilizer element (V) is more concentrated in the β phase. The metallograph of TC4 is shown in Fig. 4(b). The spherical part is primary α phase, and the strip structure is β phase.

Ti40 is a new excellent burn resistant titanium alloy, and is often used in the case which is one of the core components of the aero engine[8]. The main causes of the excellent high thermal stability are: belonging to β titanium alloy and suitable elements evenly distributed in the pure β phase. And the metallograph of Ti40 is shown in Fig. 4(c).

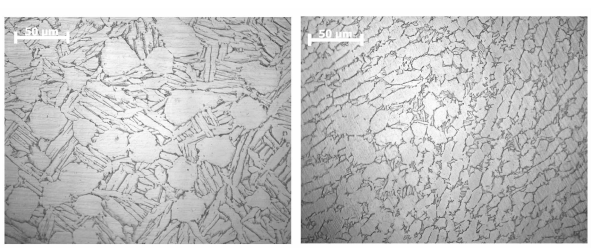

(a) Ti60 (b) TC4

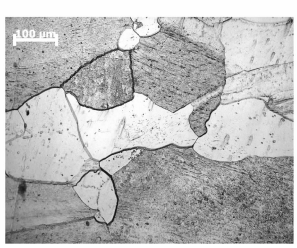

(c) Ti40

Fig. 4 Metallic phases of titanium alloys

1.4 Selection of processing parameters and electrolyte

Before the relationship between current density and surface roughness is determined, the main ECM parameters and the components of the electrolyte should be selected. Because there are many common features in ECM for titanium alloys, Ti40 has be chosen for mainly parameters selected.

1.4.1 Selection of parameters

First, the voltage needed for ECM of titanium alloys is relatively large. Because titanium is a very strongly passive metal, it is easy to form a passivation film, which will lead to an increase in the decomposition voltage during the process. Second, when a DC power supply is used, the ECM products of titanium alloys mostly form an insoluble floc that is easily adhered to the anode, leading to dissolution in different ways at the surface or the substrate of the anode. However, when a pulsed power supply is used, there is sufficient time for undissolved floc to be removed in the electrolyte at low potential. Also, corrosion of the titanium surface by the electrolyte is controlled, reducing other chemical reactions, so it is possible to obtain good surface roughness. Fig. 5 shows Ti40 surfaces processed with the main parameters shown in Tables 1,2.

Table 1 Parameters of ECM with pulsed power supply

Electrolyte concentration	Voltage/ V	Frequency/ kHz	Duty cycle	Temperature/ ℃	Feed rate/ (mm·min^{-1})
12% NaCl	30	1	0.5	40	1

Table 2 Parameters of ECM with DC power supply

Electrolyte concentration	Voltage/ V	Temperature/ ℃	Feed rate/ (mm·min^{-1})
12% NaCl	30	40	1

As can be seen from Fig. 5, ECM with pulse power produces a better surface than ECM with DC power. The surface roughness *Ra* in Fig. 5(a) is about 0.35 μm, and the surface in Fig. 5(b) is covered with a layer of yellow oxide film. The main reason is that when DC power is used, the product is not taken away immediately by the electrolyte and gradually accumulates on the anode surface. The electrolyte of the upper oxide film is more sufficiency than that of the lower oxide film, and the charge distribution also differs between the upper and lower of the oxide film. As a result, a variety of corrosion products are produced. The composition of the oxide film is shown in Table 3, from which it can be seen that it contains not only a large amount of oxygen, but also some titanium and vanadium. For Ti40, the yellow oxide film is V_xO_y or Ti_xO_y, all of which have low electrical conductivities. A short circuit can easily occur during the process. Therefore, pulse power is a better choice than DC power.

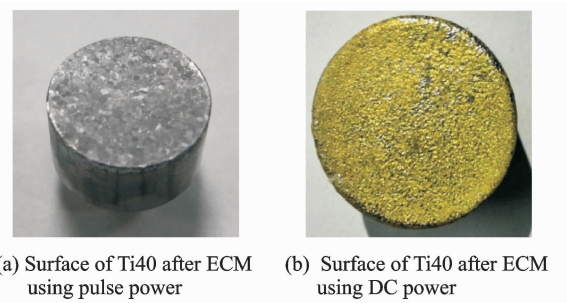

(a) Surface of Ti40 after ECM using pulse power (b) Surface of Ti40 after ECM using DC power

Fig. 5 Surfaces of Ti40 after ECM using pulse power and DC power

Table 3 Composition of oxide film of Ti40 after ECM using DC power

Composition	Atomic number	Atom/%
O	8	61.61
Ti	22	24.56
V	23	7.49
Cr	24	2.15
Cl	17	2.73
Na	11	1.46
Total		100.00

1.4.2 Selection of electrolyte

The passivation film which has poor electrical conductivity is very dense and firmly adhered to the surface of the anode. Titanium and its alloys are difficult to dissolve because of the passivation film. But the passivation can be activated when the electrolyte contains certain anions, especially halide ions. In order of activation ability, these anions are $Br^- > Cl^- > I^- > ClO_3^- > NO_3^- > SO_4^{2-}$. Therefore, electrolytes based on anions that do not contain oxygen are generally

used for ECM of titanium alloys. Thus, the halide salts sodium chloride and sodium bromide are used in preference to the oxo-anion salts sodium chlorate and sodium nitrate, because a titanium oxide film is rarely generated in these electrolytes.

As shown in Fig. 6, when Ti40 is machined using a sodium nitrate electrolyte with the main parameters shown in Table 4, the surface roughness Ra in Fig. 6(a) is about 0.32 μm and the surface using sodium nitrate electrolyte is covered with a layer of black oxide film in Fig. 6(b). In addition, the surface roughness in Fig. 6(b) is greater than the range of the instrument which range is up to 10 μm. Therefore, a sodium nitrate electrolyte is not suitable for ECM of titanium alloys, and, in practice, sodium chloride is generally used.

Table 4 Parameters of ECM with $NaNO_3$/NaCl electrolyte

Electrolyte concentration	Voltage/V	Frequency/kHz	Duty cycle	Temperature/℃	Feed rate/(mm·min^{-1})
20% $NaNO_3$/NaCl	40	1	0.5	40	1

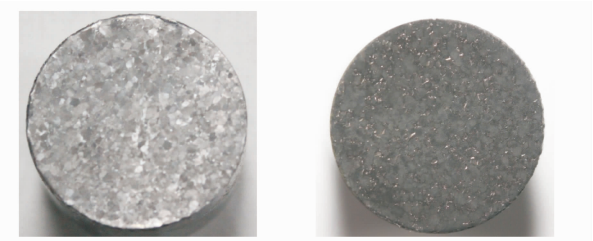

(a) Surface of Ti40 after ECM using sodium chloride (b) Surface of Ti40 after ECM using sodium nitrate electrolyte

Fig. 6 Surfaces of Ti40 after ECM using sodium chloride and sodium nitrate electrolyte

2 Experiments and Results

Experiments are performed to determine the relationship between current density and roughness and to reveal the surface morphology. The parameters shown in Table 1 are used, except that when analyzing the effect of current density on roughness, the feed rate is varied. The reason is that, for the same material and electrolyte, the product of current efficiency η and electrochemical equivalent ω (cm^3/(A · min)) is basically the same, so the corrosion rate in the normal direction, v_a(mm/min), has a linear relationship with the current density i(A/cm^2)

$$v_a = \eta\omega i \tag{1}$$

2.1 Experiments investigating relationship between current density and surface roughness

First, to obtain the relationship between the current density and the surface roughness of titanium alloys subjected to ECM, a large number of experiments are carried out. Figs. 7—9 show the variation of surface roughness with current density. The machining parameters are as in Table 1 except for the feed rate, which varied from 0.5 mm/min to 1.5 mm/min. Additionally, each experimental result is tested three times to increase the reliability of the tests. Acquisition system based on virtual instrument for current signal is established, and the values of the current are obtained from current hall sensor. When the machining goes to balance, the accurate current density can be obtained by the actual current and the processing area

$$i = \frac{I}{B} \tag{2}$$

where i(A/cm^2) is the current density, I(A) the actual current, and B(cm^2) the processing area.

Fig. 7 shows that in the sodium chloride electrolyte system, the surface roughness of Ti60 is relatively good at low current density. However, when the current density is more than 80 A/cm^2, the roughness increases considerably. Therefore, a relatively low current density should be used for ECM of Ti60. From Fig. 8, it can be seen that the surface roughness of TC4 is about 0.30 μm at low current densities, and it increases slightly with current density increasing. Therefore, high current densities can be employed for ECM of TC4. Fig. 9 shows that the surface roughness of Ti40 is about 0.3 μm at low current densities and decreases slightly as the current density increases, until dropping rather more sharply to a minimum of 0.28 μm at 75 A/cm^2, before increasing again (but not to very large values). Therefore, high current densities can also be applied for ECM of Ti40.

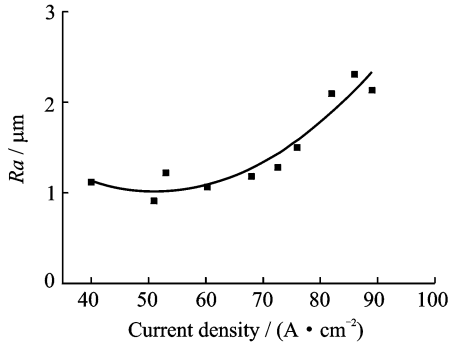

Fig. 7 Effect of current density on Ti60 surface roughness

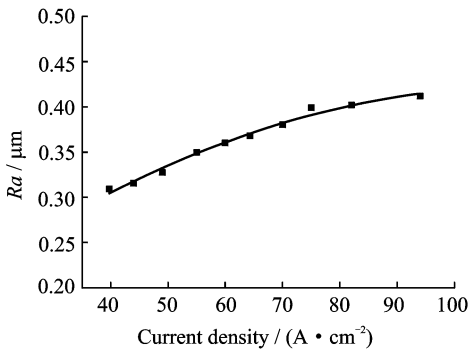

Fig. 8 Effect of current density on TC4 surface roughness

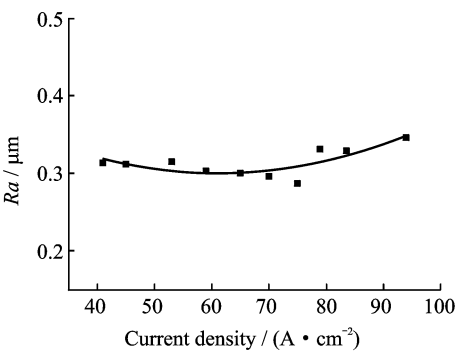

Fig. 9 Effect of current density on Ti40 surface roughness

2.2 Surface morphology

To determine the surface morphology, ECM experiments are carried out for the three different titanium alloys at the same feed rate. The machining parameters are shown in Table 1. The surface morphology is observed by a scanning electron microscope (SEM; Hitachi, S3400N, Japan). Fig. 10 shows SEM bright images of the alloys.

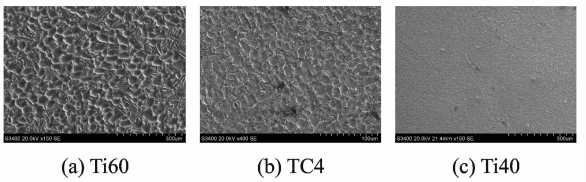

Fig. 10 SEM images showing surface morphology of titanium alloys subjected to ECM

From Figs. 10(a,b), it can be observed that a material metallographic morphology appears on the surfaces of Ti60 and TC4 after machining. In contrast to the general metallographic morphology, the α phase appears as concave, while the β phase and transformed β structure emerge as convex after ECM. It is clear that the pits in Ti60 are deeper. From Fig. 10(c), it can be seen that there are no grain boundaries on the surface of Ti40, which is relatively smooth.

To compare the depths of the concavities on the surfaces of the different titanium alloys after ECM, their three-dimensional surface topography is examined, and the three alloys are each processed at two different current densities.

Fig. 11 shows the three-dimensional surface topography of the three titanium alloys after ECM, observed by a three-dimensional video microscope (Leica DVM5000, Germany), with the machined surface roughness being measured by a surface roughness tester with 0.01 μm accuracy (Perthometer Mahr1, Germany). The machining parameters are shown in Table 1 except that the feed rate is varied.

From Fig. 11, it can be obtained that the surface roughness of Ti60 after ECM is significantly worse than that of Ti40 and TC4. For Ti60, the surface roughness is 1.239 μm at a current density of 40 A/cm^2, and it is 1.843 μm at 80 A/cm^2. It is confirmed that the higher the current density is, the lower the amount of α phase is. Fig. 12 shows the concavities in the Ti60 surface more clearly.

For TC4, at a current density of 40 A/cm^2, the surface roughness is 0.317 μm, and at 80 A/cm^2, it is 0.388 μm. For Ti40, at 40 A/cm^2, the

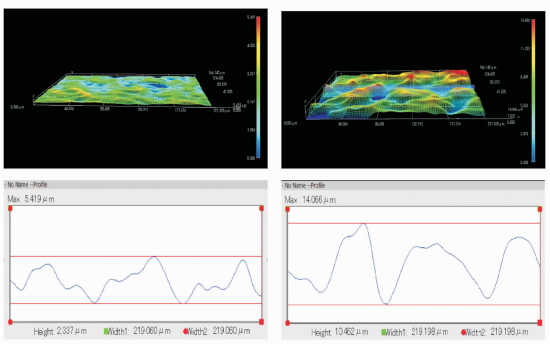

i=40 A / cm^2(Ra=1.239 μm) i=80 A / cm^2(Ra=1.843 μm)

(a) Ti60

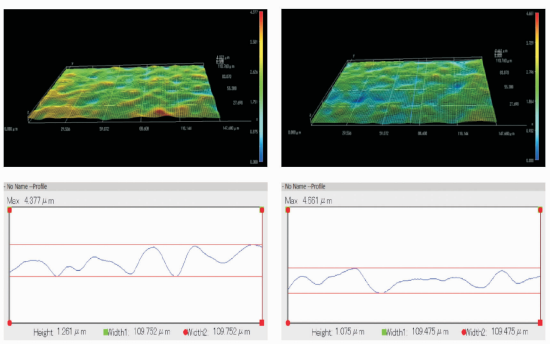

i=40 A / cm^2(Ra=0.317 μm) i=80 A / cm^2(Ra=0.388 μm)

(b) TC4

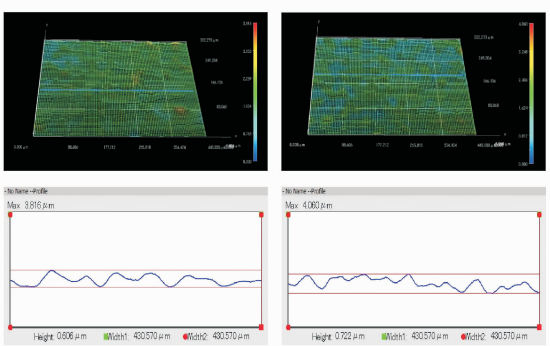

i=40 A / cm^2(Ra=0.331 μm) i=80 A / cm^2(Ra=0.347 μm)

(c) Ti40

Fig. 11 Surfaces topography of titanium alloys at different current densities

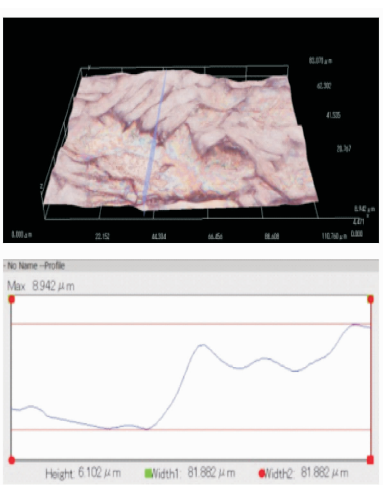

Fig. 12 Surface morphology of Ti60 after ECM

surface roughness is 0.331 μm, and at 80 A/cm^2, it is 0.347 μm. It can thus be seen that the surface roughness of TC4 and Ti40 increases slightly with increasing current density.

3 Analysis

Based on the above experimental results, the characteristics of the surface morphology of Ti60, Ti40, and TC4 after ECM can be analyzed. At the same time, the relationship between the surface roughness and the current density can be further analyzed in terms of the phases and composition of the materials.

The microstructure morphology of Ti60 after ECM is shown in Fig. 10(a). The transformed β structures are convex and the α phases concave. The corrosion rates of the two structures are different, which can be considered to result from the different electrochemical equivalents in the two phases. The possible causes of these different electrochemical equivalents may be as follows: the α-phase stabilizer element (Al) is more concentrated in the α phase, while the β-phase stabilizer elements (Mo, Si) are more concentrated in the transformed β structures. The rare-earth element Nd, which is often present between the two structures but generally not within them, plays the role of fine-grain strengthening by reducing the activation energy of the grains and preventing grain growth. Therefore, it generally does not affect the electrochemical equivalents of the two structures. Neutral elements (Sn, Zr) have good solubility in both structures.

Different substitutional elements are rich in the two different structures and have different electrochemical equivalents, resulting in different corrosion rates of the two phases. Electrochemical equivalent ω can be determined by the relative atomic mass A, valence n, density ρ(g/cm^3) and Faraday constant F (1 608.3 A · min/mol)

$$\omega = \frac{A}{n\rho F} \tag{3}$$

In ECM of Ti60, the surface roughness in-

creases with the current density as shown in Fig. 7. The electrochemical equivalents of the substitutional elements present in Ti60 are shown in Table 5. As can be seen from Eq. (1), the values of $\eta\omega$ of adjacent phases differ. The differences in rates between the phases will be enlarged with the current density increasing, which results in a worse roughness.

Table 5 Electrochemical equivalents of substitutional elements in Ti60

Type	Element	ω/ $(cm^3 \cdot (A \cdot min)^{-1})$
α-phase stabilizer element	Al	0.002 1(3+)
Neutral elements	Sn	0.005 0(2+);0.002 5(4+)
	Zr	0.002 2(4+)
β-phase stabilizer elements	Mo	0.001 0(6+)
	Si	0.001 9 (semiconductor)
	Nd	

In TC4, the electrochemical equivalent of Al is 0.002 1 $cm^3/(A \cdot min)$ in the α phase, and those of the different oxidation states of V are 0.002 6 (2+), 0.001 7 (3+), 0.001 3 (4+), and 0.001 0 (5+) $cm^3/(A \cdot min)$ in the β phase, as shown in Table 6. On the other hand, in Ti60, the electrochemical equivalent of Mo is 0.001 0 (6+) $cm^3/(A \cdot min)$ in the β phase and that of Al is 0.002 1 $cm^3/(A \cdot min)$ in the α phase. Based on these data, the differences in the electrochemical equivalents of substitutional elements in Ti60 are more evident than in TC4. Furthermore, as noted in Table 5, Si is a semiconductor, and is difficult to corrode by ECM. Thus, Ti60 differs from TC4 not only in the electrochemical equivalents of substitutional elements in the different phases, but also in the presence of Si, which is resistant to ECM. Meanwhile, the grain of TC4 is smaller than that of Ti60. Under the same processing area, the elements in TC4 are more uniform than those in Ti60. Thus, difference of the elements' electrochemical equivalent in TC4 is relatively less than that in Ti60. Therefore, TC4 has a better surface roughness than Ti60 after ECM.

Table 6 Electrochemical equivalents of substitutional elements in TC4

Type	Element	ω/ $(cm^3 \cdot (A \cdot min)^{-1})$
α-phase stabilizer element	Al	0.002 1 (3+)
β-phase stabilizer element	V	0.002 6 (2+); 0.001 7 (3+); 0.001 3 (4+); 0.001 0 (5+)

It can be seen from Fig. 9 and Fig. 10(c) that in the sodium chloride electrolyte system, the surface roughness of Ti40 is good and that as the current density increases, the roughness increases only slightly. The reason is that the electrochemical equivalents of the substitutional elements in the adjacent phases are approximately equal. Ti40 is a wholly β-phase titanium alloy. Because Cr and V are evenly distributed in the grains, there is no difference between phases. The electrochemical equivalent does not differ between the phases, as shown in Table 7, so the corrosion is more even, and a good surface roughness is obtained. Therefore, we can choose a relatively high current density for processing Ti40.

Table 7 Electrochemical equivalents of substitutional elements in Ti40

Type	Element	ω/ $(cm^3 \cdot (A \cdot min)^{-1})$
β-phase stabilizer elements	Cr	0.001 5 (3+); 0.000 8 (6+)
	V	0.002 6 (2+); 0.001 7 (3+); 0.001 3 (4+); 0.001 0 (5+)

4 Conclusions

We focus on the investigation of dissolution characteristics in new titanium alloys for the aerospace industry. By analyzing the composition and microstructure of different alloys, an appropriate range of current density can be proposed for a good surface roughness. With this approach, the following conclusions can be obtained:

(1) The experimental results show that, compared with TC4 and Ti60, ECM of Ti40 gives better results in terms of surface roughness. For Ti60, Ra is in the range of 0.910—2.418 μm at current densities ranging from 40 A/cm^2 to

100 A/cm^2; for TC4, Ra is about 0.309—0.411 μm at 40—100 A/cm^2; and for Ti40, Ra is about 0.30 μm at 40—100 A/cm^2 (and as low as 0.28 μm at 75 A/cm^2).

(2) Comparing two-phase(or two-structure) and single-phase titanium alloy, it can be seen that it is easier to obtain a good surface roughness after ECM of the latter. In the case of the α+β titanium alloy and near-α titanium alloy, because of the different substitutional elements in the different phases, the electrochemical equivalent volumes also differ between phases. Therefore, at the same ECM current density, the surface roughness of the α+β titanium alloy and near-α titanium alloy is worse than that of the single-phase alloy.

Acknowledgements

This work was supported by the National Natural Science Foundation of China (No. 51205199), the Program for New Century Excellent Talents in University (No. NCET-12-0627), the Funding of Jiangsu Innovation Program for Graduate Education (No. CXLX13_141), and the Fundamental Research Funds for the Central Universities.

References:

[1] CHEN Y, DING L Y, FU Y C, et al. Dry grinding of titanium alloy using brazed monolayer CBN wheels coated with graphite lubricant[J]. Transactions of Nanjing University of Aeronautics & Astronautics, 2014,31(1):104-110.

[2] SHI Q, HE N, LI L, et al. Analysis on surface integrity during high speed milling for new damage-tolerant titanium alloy[J]. Transactions of Nanjing University of Aeronautics & Astronautics, 2012,29(3):222-226.

[3] WANG X D, LI Y H, LI Q P, et al. Property and thermostablity study on TC6 titanium alloy nanostructure processed by LSP[J]. Transactions of Nanjing University of Aeronautics & Astronautics, 2012,29(1):68-76.

[4] PRAMANIK A. Problems and solutions in machining of titanium alloys[J]. Int J Adv Manuf Technol, 2014,70(5/6/7/8):919-928.

[5] PAUL G, ROY S, SARKAR S. Investigations on influence of process variables on crater dimensions in micro-EDM of gamma-titanium aluminide alloy in dry and oil dielectric media[J]. Int J Adv Manuf Technol, 2013,65(5/6/7/8):1009-1017.

[6] KLOCKE F, LUNG D, ARFT M. On high-speed turning of a third-generation gamma titanium aluminide[J]. Int J Adv Manuf Technol, 2013,65(1/2/3/4):155-163.

[7] JIA W J, ZENG W D, LIU J R, et al. Influence of thermal exposure on the tensile properties and microstructures of Ti60 titanium alloy[J]. Mater Lett, 2011,530(12):511-518.

[8] WANG M M, ZHAO Y Q, ZHOU L, et al. Study on creep behavior of Ti-V-Cr burn resistant alloys [J]. Mater Lett, 2004,58(26):3248-3252.

[9] FAN Z W, HONG L W, LIN M Y, et al. Experimental investigation on the influence of electrochemical micro-drilling by short pulsed voltage[J]. Int J Adv Manuf Technol, 2012,61(9/10/11/12):957-966.

[10] WANG W, ZHU D, QU N S, et al. Effects of electrode insulation thickness on electrochemical drilling [J]. Transactions of Nanjing University of Aeronautics & Astronautics, 2009,26(3):163-169.

[11] RAJURKAR K P, ZHU D, MCGEOUGH J A, et al. New development in ECM[J]. Ann CIRP, 1999, 48(2):569-579.

[12] RISKO D G. Manufacturing applications and productivity limitations of electrochemical machining[J]. Manuf Sci Eng, 1993,64:701-711.

[13] WALTHER B, SCHILM J, MICHAELIS A, et al. Electrochemical dissolution of hard metal alloys[J]. Electrochem Acta, 2007,52(27):7732-7737.

[14] KOZAK J. Mathematical models for computer simulation of electrochemical machining processes[J]. J Mater Process Technol, 1998,76(97):170-175.

[15] MUKHERJEE R, CHAKRABORTY S. Selection of the optimal electrochemical machining process parameters using biogeography-based optimization algorithm[J]. Int J Adv Manuf Technol, 2013,64(5/6/7/8):781-791.

[16] SHIRISH D, DHOBE B, DOLOI B. Surface characteristics of ECMed titanium work samples for biomedical applications[J]. Int J Adv Manuf Technol, 2011,55(1/2/3/4):177-188.

[17] DHOBE S D, DOLOI B, BHATTACHARYYA B. Analysis of surface characteristics of titanium during ECM[J]. Int J Mach Mach Mater, 2011,10(4):293-

309.

[18] LOZANO-MORALES A, GEBHART L, INMAN M, et al. Medical device surface finishing by ECM [J]. J Appl Surf Fin, 2007,2(3):192-197.

[19] ZHANG Meili. Foundation study on electrochemical machining titanium[D]. Nanjing: Nanjing University of Aeronautics and Astronautics, 2008. (in Chinese)

[20] KLOCKE F, ZEIS M, KLINK A. Experimental research on the electrochemical machining of modern titanium- and nickel-based alloys for aero engine components[J]. Procedia CIRP, 2013(6):368-372.

[21] SHULEPOV A P, KAPTSOV A V, SHMANEV V A, et al. Characteristics of electrochemical machining of titanium alloy by a sectional cathode under conditions of interruption of the process[J]. Elektronnaya Obrab Mater, 1987(5):78-81.

[22] TANG L, LI B, YANG S, et al. The effect of electrolyte current density on the electrochemical machining S-03 material[J]. Int J Adv Manuf Technol, 2014,71(9/10/11/12):1825-1833.

Mr. **Chen Xuezhen** is a Ph. D. candidate in College of Mechanical and Electrical Engineering at Nanjing University of Aeronautics and Astronautics in China. His main research interest is electrochemical machining.

Dr. **Zhu Dong** received Ph. D. degree in College of Mechanical and Electrical Engineering at Nanjing University of Aeronautics and Astronautics in 2011. His current research interest is electrochemical machining. And his recent research has focused on the electrochemical machining of the blisk.

Prof. **Xu Zhengyang** received Ph. D. degree in College of Mechanical and Electrical Engineering at Nanjing University of Aeronautics and Astronautics in 2008. In 2016, he was elected vice president of College of Mechanical and Electrical Engineering. His current research interests are electrochemical machining and hybrid machining.

Dr. **Liu Jia** received Ph. D. degree in College of Mechanical and Electrical Engineering at Nanjing University of Aeronautics and Astronautics in 2014. His current research interest is electrochemical machining, and he is currently focusing on blade maching in aircraft engine.

Prof. **Zhu Di** received Ph. D. degree in College of Mechanical and Electrical Engineering at Nanjing University of Aeronautics and Astronautics in 1985. In 2011, he was elected to the Chinese Academy of Sciences. His current research interests are micro non-traditional machining, electrochemical machining and hybrid machining.

(Executive Editor: Xu Chengting)